

## ASYMPTOTIC BEHAVIOR OF SOLUTIONS TO A VOLTERRA INTEGRO-DIFFERENTIAL EQUATION

Z. JACKIEWICZ, M. KLAUS AND C. O'CONNOR

**1. Introduction.** It is the purpose of this paper to investigate the asymptotic behavior of the solution to the Volterra integro-differential equation (VIDE)

$$(1) \quad \begin{cases} y'(t) = \gamma y(t) + \int_0^t (\lambda + \mu t + \nu s) y(s) ds, & t \geq 0, \\ y(0) = 1, \end{cases}$$

where  $\gamma, \lambda, \mu$  and  $\nu$  are real parameters, and  $\mu + \nu \neq 0$ . Our approach is to derive asymptotic results for a related ordinary differential equation (ODE), and to deduce from these the desired results for the VIDE. Equation (1) is of interest in testing the stability properties of numerical methods for VIDEs (see [3] for work along these lines). We have chosen in (1) the familiar nonconvolution kernel suggested, for example, in [1, Equation (1.5)].

Bakke and Jackiewicz [3] used an extension of the theory of difference equations of Poincaré type, developed in [2], to derive conditions under which approximate solutions to the test equation (1), resulting from applying reducible linear multistep methods and modified multilag methods, are bounded. To judge the quality of numerical methods based on this information, we should compare the behavior of the exact solution of (1) with the behavior of the corresponding numerical solution. In this paper we derive sufficient conditions for boundedness of the exact solution which allow this comparison to be made.

That (1) has a unique solution is a straightforward consequence of the smoothness of the kernel. Repeated differentiation shows that this solution also satisfies the differential equation with variable coefficients

$$(2) \quad y''' = \gamma y'' + (\lambda + (\mu + \nu)t)y' + (2\mu + \nu)y.$$

In §2 and §3 we find three solutions to (2) in the form of contour integrals parametrized by  $t$ . An extension of Laplace's method for

---

The work of the first-named author was supported by the National Science Foundation under grant NSF DMS - 8520900.

contour integrals is then used, in which the effect of a dominant factor of the integrand is shown to be governed by a saddle point, to derive the asymptotic behavior of these solutions. We refer the reader to Olver [7, Sections 4.6 and 9.2] for a discussion of these methods (Bender and Orzag [4] provide a more elementary treatment; see also Henrici [6]). The three contour integrals display distinct asymptotic behaviors and hence are linearly independent. Thus, the solution of (1) is a linear combination of these. Unfortunately, we cannot find the coefficients of the linear combination explicitly in general, and so we cannot establish the asymptotic properties of (1) directly from those of (2). In spite of this, we can show that all solutions of (2) are bounded once  $\gamma < 0$ ,  $\mu + \nu < 0$  and  $2\mu + \nu < 0$ . It follows that under these conditions the solution of (1) is also bounded. This fact is a strengthened form of a conjecture in [3] and is sufficient for the needs of the numerical investigation.

We note that the asymptotic analysis of (2) is related to that of Airy's equation (Olver [7]) and more closely to that of the generalized Airy functions considered by Drazin and Reid [5] in their appendix. When  $\mu/(\mu + \nu)$  is a nonnegative integer, two linearly independent solutions of (2) may be expressed as finite linear combinations of Drazin and Reid's integrals.

In §4 we compare two numerical methods having different stability regions with respect to equation (1). One of the stability regions contains the stability region of (1) itself, while the other does not. We demonstrate that the method with the larger stability region can successfully integrate an inhomogeneous VIDE with homogeneous part as in (1) for a large selection of parameter values.

**2. Integral representation of solutions.** We now seek solutions of (2) in the form

$$(3) \quad y(t) = \int_{\Gamma} e^{t\xi} \psi(\xi) d\xi, \quad t \geq 0,$$

where  $\Gamma$  is a contour in the complex plane and  $\psi$  is an analytic function to be determined. Substituting (3) into (2) and using integration by parts we obtain

$$\begin{aligned} & \int_{\Gamma} (\xi^3 - \gamma\xi^2 - \lambda\xi - (2\mu + \nu))e^{t\xi}\psi(\xi) d\xi \\ &= (\mu + \nu)e^{t\xi}\xi\psi(\xi)|_{\partial\Gamma} \\ & \quad - (\mu + \nu) \int_{\Gamma} e^{t\xi} \frac{d}{d\xi}(\xi\psi(\xi)) d\xi. \end{aligned}$$

Here  $\partial\Gamma$  stands for the “boundary” of  $\Gamma$ . If we assume that

$$(4) \quad e^{t\xi}\xi\psi(\xi)|_{\partial\Gamma} = 0,$$

we are led to consider an  $\psi$  that satisfies the differential equation

$$(\mu + \nu)\xi\psi'(\xi) + (\xi^3 - \gamma\xi^2 - \lambda\xi - \mu)\psi(\xi) = 0.$$

Since we are assuming that  $\mu + \nu \neq 0$ , the unique solution of this equation, up to a constant factor, is given by

$$(5) \quad \psi(\xi) = \xi^{\beta} \exp\left\{A\frac{\xi^3}{3} + B\frac{\xi^2}{2} + C\xi\right\},$$

where  $A = -1/(\mu + \nu)$ ,  $B = \gamma/(\mu + \nu)$ ,  $C = \lambda/(\mu + \nu)$  and  $\beta = \mu/(\mu + \nu)$ . It follows that (3) gives a solution of (2) with this choice of  $\psi$  and any contour  $\Gamma$  satisfying (4) for which the integrand is integrable. In the next section we give several choices for the contour  $\Gamma$  which lead to three linearly independent solutions of (2) and we use the ideas of the method of steepest descent and Laplace’s method to determine the asymptotic behavior of (3) for these choices.

**3. Asymptotic behavior of solutions.** Before we embark on the asymptotic analysis, a few remarks on Laplace’s method are in order. In studying the asymptotic behavior of the integral

$$\int_{\Gamma} e^{tg(\xi)}h(\xi) d\xi, \quad t \rightarrow \infty,$$

the main challenge is to account for cancellation that occurs due to the rapidly changing argument of the integrand as  $t$  increases. A paradigm of such cancellations is the Riemann-Lebesgue lemma (Olver [7]). The idea behind the method of steepest descent is that, when

$g$  and  $h$  are analytic, the contour  $\Gamma$  may be deformed with the aid of Cauchy's theorem into a contour  $\Gamma^*$  on which the imaginary part of  $g$  is constant, thus eliminating the problem of cancellations. Now, and this is the key idea in Laplace's method, the integral is typically dominated by the integral along any nonempty subset of  $\Gamma^*$  of the form  $\{\omega \in \Gamma^* : \operatorname{Re} g(\omega) > \text{constant}\}$ . Unfortunately, these methods do not apply directly here. However, by staying on a steepest descent path for a dominant part of the exponent, the same ideas may be exploited; Olver [7, §9.2], gives the details of this approach.

Returning to the integral (3), with  $\psi$  as in (5), let us make the change of variables  $\omega = |A|^{\frac{1}{3}}\xi$  and set  $s = t|A|^{-\frac{1}{3}}$ ,  $y^*(s) = y(t)$ ,  $b = B|A|^{-\frac{2}{3}}$ , and  $c = C|A|^{-\frac{1}{3}}$ . As a result we get

$$(6) \quad y^*(s) = |A|^{-(\beta+1)/3} \int_{\Gamma} e^{s\omega} \omega^{\beta} \exp\left\{\operatorname{sign}(A)\frac{\omega^3}{3} + b\frac{\omega^2}{2} + c\omega\right\} d\omega,$$

where  $\Gamma$  now denotes a new contour. It is clear that we must consider separately the two cases determined by the sign of  $A$ . In the following, for notational convenience,  $D$  denotes a nonzero complex constant, but not necessarily the same one even on a given line. To denote a small positive number we use  $\varepsilon$ . The notation  $a(t) \sim b(t)$  is used to mean that  $a(t)/b(t) \rightarrow 1$  as  $t \rightarrow \infty$ .

*Case 1.*  $A < 0$ . In this case, formula (6) may be written

$$(7) \quad y^*(s) = D \int_{\Gamma} \omega^{\beta} \exp\{f_s(\omega)\} d\omega,$$

where

$$f_s(\omega) = s\omega - \frac{\omega^3}{3} + b\frac{\omega^2}{2} + c\omega.$$

For  $s$  sufficiently large the saddle points of  $f_s$  are real and are given by

$$\omega_{\pm} = \frac{b}{2} \pm \sqrt{c + s + b^2/4} \sim \pm\sqrt{s}.$$

The expansions of  $f_s$  about each of these points are given succinctly by (8)

$$f_s(\omega) = f_s(\omega_{\pm}) - \omega_{\pm}^3 \left[ \left(\frac{\omega}{\omega_{\pm}} - 1\right)^2 + \frac{1}{3} \left(\frac{\omega}{\omega_{\pm}} - 1\right)^3 \right] + \frac{b}{2} \omega_{\pm}^2 \left(\frac{\omega}{\omega_{\pm}} - 1\right)^2.$$

Routine algebraic manipulation leads to the useful result that

$$(9) \quad f_s(\omega_{\pm}) = \pm \frac{2}{3}s^{3/2} \pm \left(c + \frac{b^2}{4}\right)s^{1/2} + \frac{b}{2}s + \frac{b}{12}(b^2 + 6c) + o(1),$$

where  $o(1)$  is a function that goes to zero as  $s \rightarrow \infty$ .

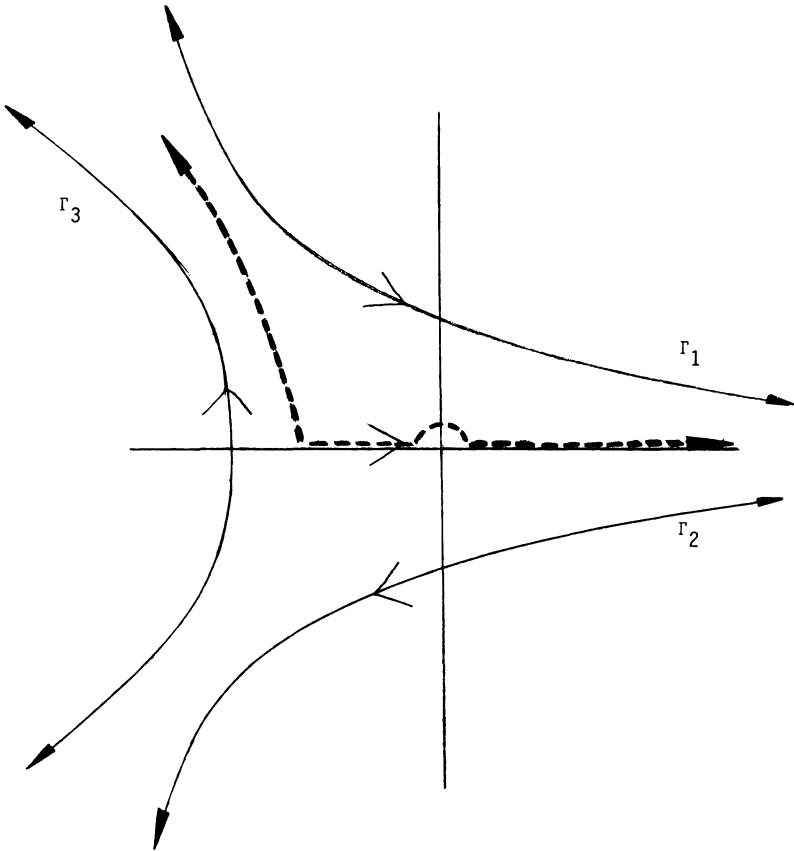


FIGURE 1.

We consider three types of contour, which are illustrated in Figure 1. A contour of type  $\Gamma_1$  is asymptotically parallel to a ray of angle

between  $-\pi/6$  and  $+\pi/6$  on one side and asymptotically parallel to a ray of angle between  $\pi/2$  and  $5\pi/6$  on the other. A contour of type  $\Gamma_2$  is the reflection of one of type  $\Gamma_1$  in the  $x$ -axis. A contour of type  $\Gamma_3$  is asymptotically parallel to a ray of angle between  $\pi/2$  and  $5\pi/6$  in the upper half-plane and is symmetric in the  $x$ -axis. We assume that these contours bear the relation to the origin indicated in Figure 1 and that the integrand of (7) is integrable along each. There exist such contours since the term  $-\omega^3/3$  has a large negative real part that strongly dominates the exponent along all the asymptotes allowed. From Cauchy's Theorem, and from the dominance of  $-\omega^3/3$ , we see that the integral (7) is the same along any two contours of the same type. Thus, in writing integrals below, we need not specify a choice of contour and may simply say "the contour  $\Gamma_1$ ." Condition (4) is satisfied for each type of contour and so (7) does represent a solution of (1) for each type.

Consider first the integral over  $\Gamma_1$ . Let us substitute  $\eta = \omega/\omega_+$ , set  $\tau = \omega_+^3$ , and apply (8) to get this solution of (2)

$$(10) \quad \begin{aligned} y_1^*(s) = & D\omega_+^{\beta+1} \exp\{f_s(\omega_+)\} \\ & \cdot \int_{\Gamma_1} \eta^\beta \exp\left\{-\tau\left[(\eta-1)^2 + \frac{1}{3}(\eta-1)^3\right]\right\} \\ & \cdot \exp\left\{\frac{b}{2}\tau^{2/3}(\eta-1)^2\right\} \cdot d\eta. \end{aligned}$$

Note that a scale change of a contour of any of the three types yields a contour of the same type. By following the steepest descent paths of the function  $-(\eta-1)^2 - \frac{1}{3}(\eta-1)^3$ , we can find a contour of type  $\Gamma_1$  which contains  $[1/2, \infty)$  on which this function is maximal at  $\eta = 1$  and only approaches this maximum at  $\eta = 1$ . This contour is represented by the dotted line in Figure 1. Using it as our choice of  $\Gamma_1$  we have the following calculation, in which the method of Olver's [7, Theorem 9.2.1] allows us to ignore the  $\tau^{2/3}$  term in the exponent of the integrand and Laplace's method for contour integrals (Olver [7, Theorem 4.6.1]) may be used to justify the final result:

$$\begin{aligned}
& \int_{\Gamma_1} \eta^\beta \exp\left\{-\tau\left[(\eta-1)^2 + \frac{1}{3}(\eta-1)^3\right]\right\} \cdot \exp\left\{\frac{b}{2}\tau^{2/3}(\eta-1)^2\right\} d\eta \\
& \sim \int_{1/2}^{3/2} \eta^\beta \exp\left\{-\tau\left[(\eta-1)^2 + \frac{1}{3}(\eta-1)^3\right]\right\} d\eta \\
& \sim \int_{-\infty}^{+\infty} \exp\{-\tau(\eta-1)^2\} d\eta = \sqrt{\pi/\tau}.
\end{aligned}$$

From this and (10) we see that

$$y_1^*(s) \sim D s^{(\beta+1)/2} \exp\{f_s(\omega_+)\} / \sqrt{\tau} \sim D s^{(2\beta-1)/4} \exp\{f_s(\omega_+)\}.$$

The asymptotic result (9) may now be used to deduce

$$(11) \quad y_1^*(s) \sim D s^{(2\beta-1)/4} \exp\left\{\frac{2}{3}s^{3/2} + \left(c + \frac{b^2}{4}\right)s^{1/2} + \frac{b}{2}s\right\}.$$

No new asymptotic behavior is found by considering  $\Gamma_2$  since, as for  $\Gamma_1$ , the saddle point  $\omega_+$  dominates. However, the integral along  $\Gamma_1 \cup \Gamma_2$  is different asymptotically, due to cancellation of the leading effects. A contour of type  $\Gamma_1 \cup \Gamma_2$  may be deformed into the path  $C$  given in Figure 2. This consists of a clockwise circle of radius  $\varepsilon$ , a finite interval  $(-K, -\varepsilon)$  of the negative real axis traversed in both directions, with two branches having the  $\pm 2\pi/3$ -rays as asymptotes. Consider the integral (7) over this contour, for  $\beta$  not a nonnegative integer, denoting it by  $y_2^*$ . The integral over the two branches is seen to be exponentially small in  $s$ . Applying Watson's lemma for loop integrals (Olver [7, Theorem 4.5.1]) to the integral on the remainder of the path, the following calculation may be justified, thus giving a second solution of (7) satisfying

$$\begin{aligned}
y_2^*(s) & \sim \int_C \omega^\beta \exp\left\{s\omega - \frac{\omega^3}{3} + b\frac{\omega^2}{2} + c\omega\right\} d\omega \\
& \sim \int_C \omega^\beta e^{s\omega} d\omega = \frac{2\pi i}{\Gamma(-\beta)} s^{-\beta-1} = Ds^{-\beta-1}.
\end{aligned}$$

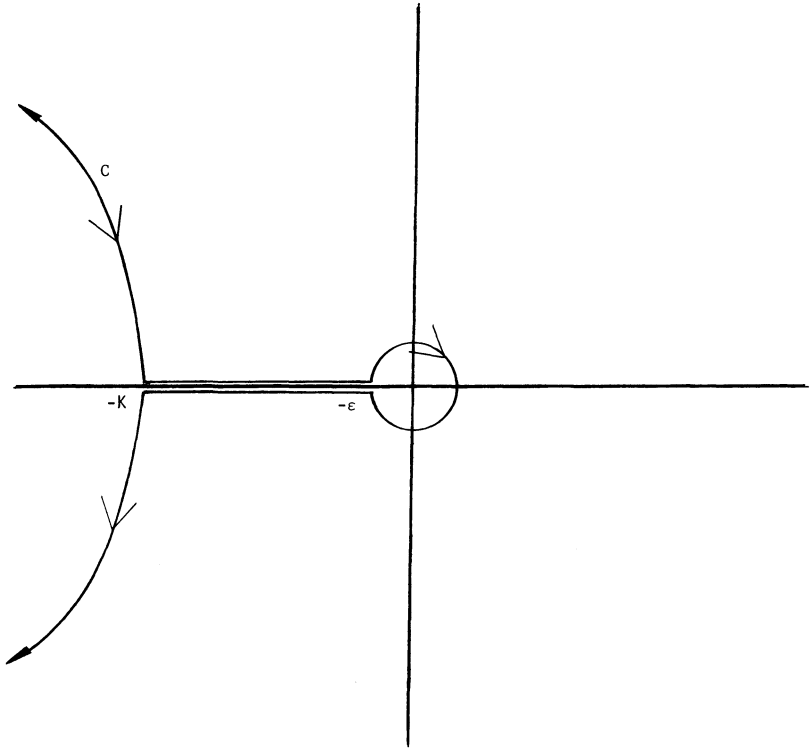


FIGURE 2.

If  $\beta$  is a nonnegative integer the integrand of (7) is analytic and so, by Cauchy's theorem, the integrals (7) over  $\Gamma_1, \Gamma_2$  and  $\Gamma_3$  are linearly dependent. In this case, the dotted contour of Figure 3 satisfies condition (4), and a standard application of Laplace's method shows again that the solution of (2) which arises in this way satisfies

$$y_2^*(s) = \int_{-\infty}^0 e^{s\omega} \omega^\beta d\omega = Ds^{-\beta-1}.$$



We have found a solution of (2) with the behavior

$$(12) \quad y_2^*(s) \sim Ds^{-\beta-1}$$

for every value of  $\beta$ .

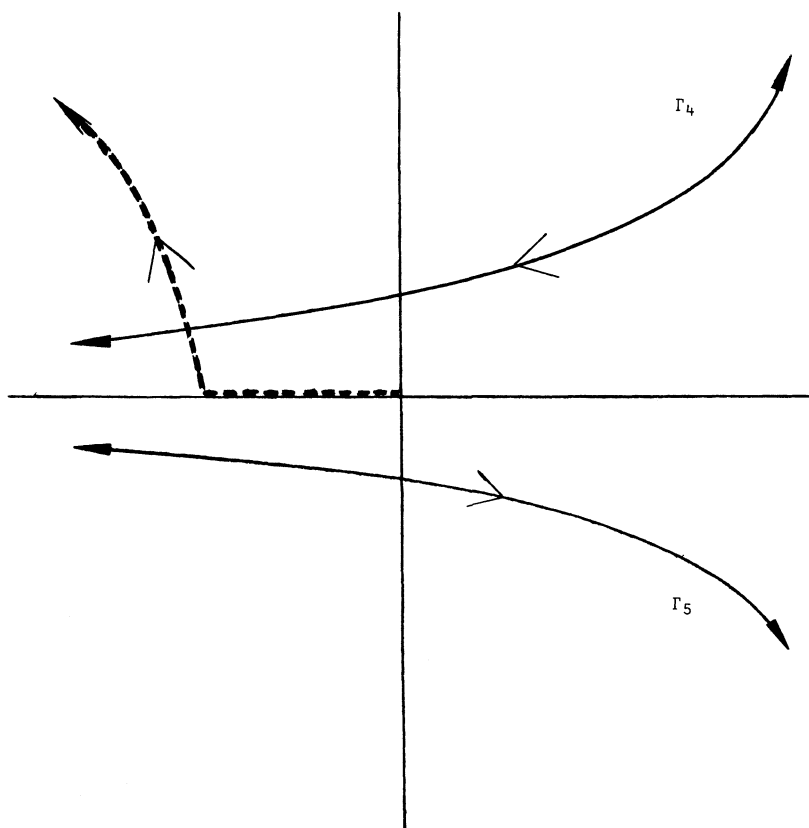


FIGURE 3.

Now consider the integral (7) along the contour  $\Gamma_3$ . Using the expansion (8), and setting  $\eta = -\omega/\omega_-$  and  $\tau = -\omega_-^3$ , we obtain a

solution

$$y_3^*(s) = D\omega_-^{\beta+1} \exp\{f_s(\omega_-)\} \int_{\Gamma_3} \eta^\beta \exp\left\{\tau\left[(\eta+1)^2 - \frac{1}{3}(\eta+1)^3\right]\right\} \\ \cdot \exp\left\{\frac{b}{2}(-\tau)^{2/3}(\eta+1)^2\right\} d\eta.$$

We may choose for  $\Gamma_3$  the path of steepest descent of  $(\eta+1)^2 - \frac{1}{3}(\eta+1)^3$  which goes vertically through the point  $-1$ . This function is real-valued on this path and attains its maximum at  $-1$ . Arguing as we did when considering  $\Gamma_1$ , we find that

$$(13) \quad y_3^*(s) \sim D\omega_-^{\beta+1} \exp\{f_s(\omega_-)\} \int_{-1-i\infty}^{-1+i\infty} \exp\{\tau(\eta+1)^2\} d\eta \\ \sim Ds^{(2\beta-1)/4} \exp\left\{-\frac{2}{3}s^{3/2} - \left(c + \frac{b^2}{4}\right)s^{1/2} + \frac{b}{2}s\right\},$$

from (9), the integral here being  $i\sqrt{\pi/\tau}$ . We have found solutions with three distinct asymptotic behaviors. These solutions must clearly be linearly independent. So the case  $A < 0$  is complete.

*Case 2.  $A > 0$ .* In this case formula (6) may be written as

$$(14) \quad y^*(s) = D \int_{\Gamma} \omega^\beta \exp\{f_s(\omega)\} d\omega,$$

where

$$f_s(\omega) = s\omega + \frac{\omega^3}{3} + b\frac{\omega^2}{2} + c\omega.$$

The saddle points of  $f_s$  are

$$\omega_{\pm} = -\frac{b}{2} \pm \sqrt{b^2/4 - c - s},$$

and the expansions of  $f_s$  about both points may again be given simultaneously:

$$(15) \quad f_s(\omega) = f_s(\omega_{\pm}) + \omega_{\pm}^3 \left[ \left(\frac{\omega}{\omega_{\pm}} - 1\right)^2 + \frac{1}{3} \left(\frac{\omega}{\omega_{\pm}} - 1\right)^3 \right] \\ + \frac{b}{2} \omega_{\pm}^2 \left(\frac{\omega}{\omega_{\pm}} - 1\right)^2.$$

As before, routine algebra leads to the asymptotic formula

$$(16) \quad f_s(\omega_{\pm}) = \pm i \left[ \frac{2}{3} s^{3/2} + \left( c - \frac{b^2}{4} \right) s^{1/2} \right] - \frac{b}{2} s + \frac{b}{12} (b^2 - 6c) + o(1),$$

where  $o(1)$  is a function that goes to zero as  $s \rightarrow \infty$ . It is important to note that  $\omega_{\pm}$  are complex now for  $s$  sufficiently large and their imaginary parts are large compared to their real parts. In fact,

$$(17) \quad \omega_{\pm} = \pm i \sqrt{c + s - b^2/(8\sqrt{s})} - b/2 + o(s^{-1}),$$

where  $s \cdot o(s^{-1}) \rightarrow 0$  as  $s \rightarrow \infty$ .

Let  $\Gamma_4$  and  $\Gamma_5$  represent the families of contours formed by reflecting contours of type  $\Gamma_1$  and  $\Gamma_2$  in the  $y$ -axis, respectively. These are illustrated in Figure 3. On such contours, the dominance of the  $\omega^3/3$  term in the exponent of the integrand in (14) will ensure integrability, and that (4) holds. Thus (14) gives a solution of (2) for each of  $\Gamma_4$  and  $\Gamma_5$ , which we denote by  $y_4^*(s)$  and  $y_5^*(s)$ , respectively. Consider first  $\Gamma_4$ . On substituting  $\eta = i\omega/\omega_+$  and setting  $\tau = i\omega_+^3$ , (14) and (15) lead to

$$(18) \quad \begin{aligned} y_4^*(s) &= D\omega_+^{\beta+1} \exp\{f_s(\omega_+)\} \\ &\cdot \int_{\Gamma_4} \eta^{\beta} \exp \left\{ \tau \left[ i(\eta - i)^2 + \frac{1}{3}(\eta - i)^3 \right] \right\} \\ &\cdot \exp \left\{ \frac{b}{2} \tau^{2/3} (\eta - i)^2 \right\} d\eta. \end{aligned}$$

Note that, for  $s$  sufficiently large, the image of a contour of type  $\Gamma_4$  or  $\Gamma_5$  under the mapping  $\eta = i\omega/\omega_+$  is again of the same type, by (17). The function  $i(\eta - i)^2 + \frac{1}{3}(\eta - i)^3$  has a path of steepest descent of type  $\Gamma_4$  through  $\eta = i$ , on which this function is real-valued and  $\eta = i$  is its only saddle point. The function takes on its maximum over the path at this point. Arguing as we did when considering  $\Gamma_1$ , we can show that the integral of (18)  $\sim D/\sqrt{\tau}$ . Now (16) and (18) together give the desired result:

$$(19) \quad y_4^*(s) \sim Ds^{(2\beta-1)/4} \exp \left\{ i \left[ \frac{2}{3} s^{3/2} + \left( c - \frac{b^2}{4} \right) s^{1/2} \right] - \frac{b}{2} s \right\}.$$

The same kind of analysis may be repeated for contours of type  $\Gamma_5$ , but it is more convenient to observe that, since the coefficients of (2)

are real, the conjugate of (19) must represent the asymptotic behavior of a different solution. Thus there is another solution satisfying

$$(20) \quad y_5^*(s) \sim Ds^{(2\beta-1)/4} \exp \left\{ -i \left[ \frac{2}{3}s^{3/2} + \left( c - \frac{b^2}{4} \right) s^{1/2} \right] - \frac{b}{2}s \right\}.$$

Finally, the methods leading to (12) may be repeated here to yield a third solution  $y_6^*$  for which

$$(21) \quad y_6^*(s) \sim Ds^{-\beta-1}.$$

This completes the case  $A > 0$ . If we now return to the notation of equation (5), we have found solutions with the following asymptotic behavior:

*Case 1.  $A < 0$ .*

$$y_1(t) \sim Dt^{(2\beta-1)/4} \exp \left\{ \frac{2}{3}|A|^{-1/2}t^{3/2} + |A|^{-1/2}(C + B^2|A|^{-1}/4)t^{1/2} + \frac{B}{2}|A|^{-1}t \right\};$$

$$y_2(t) \sim Dt^{-\beta-1};$$

$$y_3(t) \sim Dt^{(2\beta-1)/4} \exp \left\{ -\frac{2}{3}|A|^{-1/2}t^{3/2} - |A|^{-1/2}(C + B^2|A|^{-1}/4)t^{1/2} + \frac{B}{2}|A|^{-1}t \right\}.$$

*Case 2.  $A > 0$ .*

$$y_4(t) \sim Dt^{(2\beta-1)/4} \exp \left\{ i \left[ \frac{2}{3}|A|^{-1/2}t^{3/2} + |A|^{-1/2}(C - B^2|A|^{-1}/4)t^{1/2} \right] - \frac{B}{2}|A|^{-1}t \right\};$$

$$y_5(t) \sim Dt^{(2\beta-1)/4} \exp \left\{ -i \left[ \frac{2}{3}|A|^{-1/2}t^{3/2} + |A|^{-1/2}(C - B^2|A|^{-1}/4)t^{1/2} \right] - \frac{B}{2}|A|^{-1}t \right\};$$

$$y_6(t) \sim Dt^{-\beta-1}.$$

We may deduce the following from these results:

1. If  $\gamma < 0, \mu + \nu < 0$  and  $2\mu + \nu < 0$ , then all solutions of (2), and also the solution of (1), tend to zero as  $t \rightarrow \infty$ .

2. If  $\gamma < 0$  or  $\mu + \nu > 0$  or  $2\mu + \nu > 0$ , then there exists an unbounded solution of (2).

Statement 1 may be justified as follows. If  $\mu + \nu$  then  $A > 0$  and Case 2 above applies. If further we have  $\gamma < 0$  then  $B > 0$  and  $y_4(t)$  and  $y_5(t)$  tend to zero as  $t \rightarrow \infty$ . The condition  $2\mu + \nu < 0$  ensures that  $\beta + 1 > 0$  so that  $y_6(t)$  also tends to zero as  $t \rightarrow \infty$ . To justify statement 2, one may verify the following: if  $\mu + \nu > 0$  then Case 1 applies and it follows that  $y_1$  is unbounded; if  $\mu + \nu < 0$  and  $\gamma > 0$  then Case 2 applies and  $B < 0$  so that  $y_4$  and  $y_5$  are unbounded; if  $\mu + \nu < 0$  and  $2\mu + \nu > 0$  then Case 2 applies and  $y_6$  is unbounded.

**4. Numerical examples.** In this section we will compare two simple numerical methods for VIDEs of the form

$$(22) \quad \begin{cases} y'(t) = f(t, y(t), \int_0^t k(t, s, y(s)) ds), & t \geq 0, \\ y(0) = y_0, \end{cases}$$

on the basis of their behavior with respect to the test equation (1) and a related equation. For method 1 consider the Backward Euler method

$$(23) \quad y_{l+1} = y_l + hf(t_l, y_l, z_l),$$

$l = 0, 1, 2, \dots$ , where  $z_{l+1}$  is the approximation to

$$\int_0^{t_{l+1}} k(t_{l+1}, s, y(s)) ds$$

given by the composite rectangular rule of the form

$$z_{l+1} = h \sum_{j=1}^{l+1} k(t_{l+1}, t_j, y_j).$$

Here  $t_l = hl, l = 0, 1, 2, \dots$ , and  $y_l$  is the approximation to the solution  $y$  of (22) at the point  $t_l$ . For method 2 we take the Backward Euler method (23) with  $z_{l+1}$  given by the composite trapezoid rule

$$\begin{aligned} z_{l+1} = h \left\{ \frac{1}{2} k(t_{l+1}, t_0, y_0) + \sum_{j=1}^l k(t_{l+1}, t_j, y_j) \right. \\ \left. + \frac{1}{2} k(t_{l+1}, t_{l+1}, y_{l+1}) \right\}. \end{aligned}$$

It follows from the results of Bakke and Jackiewicz [3] that the stability region of method 1 is

$$S_1 = \{(h\gamma, h^2\lambda, h^3\mu, h^3\nu) : (2\mu + \nu < 0 \text{ and } \mu + \nu < 0) \\ \text{or } (2\mu + \nu > 0 \text{ and } \mu + \nu > 0)\},$$

and the stability region for method 2 is

$$S_2 = \{(h\gamma, h^2\lambda, h^3\mu, h^3\nu) : (2\mu + \nu < 0 \text{ and } \mu + \nu < 0 \\ \text{and } h^3\nu < 8 - 4h\gamma) \\ \text{or } (2\mu + \nu > 0 \text{ and } \mu + \nu > 0 \\ \text{and } h^3\nu > 8 - 4h\gamma)\},$$

To test these results experimentally, these methods were applied to the equation

$$\begin{cases} y'(t) = \gamma y(t) + \int_0^t (\lambda + \mu t + \nu s) y(s) ds + g(t), & t \geq 0, \\ y(0) = 1, \end{cases}$$

where the function  $g$  was chosen in such a way that  $y(t) = \cos(t)$  is the exact solution to this problem. This equation was then integrated on the interval  $[0, 128]$ , with a fixed stepsize  $h$ , for various choices of the parameters  $h\gamma, h^2\lambda, h^3\mu$  and  $h^3\nu$ . For  $h = 1/8$ ,  $h\gamma = -1$ ,  $h^2\lambda = -1$ , and for various choices of  $h^3\mu$  and  $h^3\nu$ , we have listed in Tables 1 and 2 the number of significant digits, defined by

$$\text{NSD}(h^3\mu, h^3\nu, t) = -\log_{10} |\text{relative error in solution at } t|,$$

for each of the two methods. The negative values of NSD indicate unstable behavior of the method for given  $(h^3\mu, h^3\nu)$ . These results are in agreement with our prediction about the stability regions of the methods under consideration. For example, the points  $(15, -7.5)$  and  $(-20, 17.5)$  belong to the stability region of method 1, but not of method 2. This is reflected in the contrasting behavior of these methods indicated in columns 3 and 7. These computations seem to indicate also that whenever the point  $(h^3\mu, h^3\nu)$  belongs to the stability region of both methods, then method 2 is more accurate than method 1 (compare columns 2, 5, 6 and 9). Both methods are unstable for  $(15, -20)$  and  $(-20, 30)$  (see columns 4 and 8).

TABLE 1  
 Numerical results for method 1:  $\text{NSD}(h^3\mu, h^3\nu, t)$

	$h^3\mu$	15	15	15	5	-20	-20	-20	-7.5
t	$h^3\nu$	30	-7.5	-20	-20	5	17.5	30	30
1	1.03	1.15	-1.49	0.79	1.07	1.93	-1.23	0.72	
2	0.74	1.03	-2.13	1.51	0.92	1.60	-1.62	2.06	
4	1.26	1.14	-2.49	1.01	1.14	1.39	-1.71	0.97	
8	0.36	0.39	-3.72	0.55	0.37	0.68	-2.66	0.59	
16	1.88	1.70	-3.50	1.60	1.76	1.44	-2.14	1.56	
32	1.43	1.39	-4.15	1.59	1.41	1.30	-2.50	1.62	
64	0.84	0.84	-5.08	0.89	0.84	0.83	-3.13	0.90	
128	1.17	1.17	-5.43	1.20	1.17	1.19	-3.18	1.20	

TABLE 2  
 Numerical results for method 2:  $\text{NSD}(h^3\mu, h^3\nu, t)$

	$h^3\mu$	15	15	15	5	-20	-20	-20	-7.5
t	$h^3\nu$	30	-7.5	-20	-20	5	17.5	30	30
1	2.69	-0.25	0.43	2.05	2.91	0.33	0.48	2.05	
2	2.84	-1.11	-0.27	2.28	3.00	-0.50	0.07	2.27	
4	2.58	-1.69	-0.67	2.95	3.13	-1.00	-0.04	2.97	
8	2.66	-3.11	-1.92	2.32	2.87	-2.33	-0.99	2.30	
16	2.80	-3.08	-1.71	2.97	2.92	-2.19	-0.47	2.98	
32	2.95	-3.92	-2.37	2.80	2.87	-2.91	-0.84	2.79	
64	2.99	-5.03	-3.30	2.76	2.87	-3.91	-1.46	2.76	
128	2.84	-5.56	-3.65	2.93	2.89	-4.32	-1.52	2.93	

## REFERENCES

1. S. Amini, C.T.H. Baker, P.J. van der Houwen and P.H.M. Wolkenfelt, *Stability analysis of numerical methods for Volterra integral equations with polynomial convolution kernels*, J. Integral Equations **5** (1983), 74-92.
2. V.L. Bakke and Z. Jackiewicz, *Boundedness of solutions of difference equations and application to numerical solution of Volterra integral equations of the second kind*, J. Math. Anal. Appl. **115** (1986), 592-605.
3. ——— and ———, *Stability analysis of reducible quadrature methods for Volterra integro-differential equations*, Apl. Math. **32** (1987), 37-48.
4. C.M. Bender and S.A. Orzag, *Advanced Mathematical Methods for Scientists and Engineers*, McGraw-Hill, New York, 1978.
5. P.G. Drazin and W.H. Reid, *Hydrodynamic Stability*, Cambridge University Press, New York, 1981.
6. P. Henrici, *Applied and Computational Complex Analysis*, Vol. 2, John Wiley, New York, 1977.
7. F.W.J. Olver, *Asymptotics and Special Functions*, Academic Press, New York, 1974.

DEPARTMENT OF MATHEMATICS, ARIZONA STATE UNIVERSITY, TEMPE, AZ 85281

DEPARTMENT OF MATHEMATICS, VPI & SU, BLACKSBURG, VA 24061

DEPARTMENT OF MATHEMATICAL SCIENCES, UNIVERSITY OF ARKANSAS, FAYETTEVILLE, AR 72701